Assessment of artery dilation by using image registration based on spatial features

E. Oubel[a], H. Neemuchwala[b], A. Hero[b], L. Boisrobert[a], M. Laclaustra[c] and A. F. Frangi[a]

[a]Computational Imaging Lab, Pompeu Fabra University, Barcelona, Spain
[b]Dept. of EECS, The University of Michigan, Ann Arbor, MI 48109-2122, USA
[c]Aragon Institute of Health Sciences, Zaragoza, Spain

ABSTRACT

The use of affine image registration based on normalized mutual information (NMI) has recently been proposed by Frangi *et al.* as an automatic method for assessing brachial artery flow mediated dilation (FMD) for the characterization of endothelial function. Even though this method solves many problems of previous approaches, there are still some situations that can lead to misregistration between frames, such as the presence of adjacent vessels due to probe movement, muscle fibres or poor image quality. Despite its widespread use as a registration metric and its promising results, MI is not the panacea and can occasionally fail. Previous work has attempted to include spatial information into the image similarity metric. Among these methods the direct estimation of α-MI through Minimum Euclidean Graphs allows to include spatial information and it seems suitable to tackle the registration problem in vascular images, where well oriented structures corresponding to vessel walls and muscle fibres are present. The purpose of this work is twofold. Firstly, we aim to evaluate the effect of including spatial information in the performance of the method suggested by Frangi *et al.* by using α-MI of spatial features as similarity metric. Secondly, the application of image registration to long image sequences in which both rigid motion and deformation are present will be used as a benchmark to prove the value of α-MI as a similarity metric, and will also allow us to make a comparative study with respect to NMI.

Keywords: Image Registration, Similarity Measures, Spatial Features, Direct Entropy Estimation, Minimal Euclidean Graphs, Flow Mediated Dilation, Vascular Ultrasound

1. INTRODUCTION

The use of affine image registration based on NMI has recently been proposed by Frangi *et al.*[1] as an automatic method for assessing brachial artery flow mediated dilation (FMD) for the characterisation of endothelial function in the diagnosis of cardiovascular diseases. Basically, this method consists in modelling changes in the artery image as an affine transformation, whose scaling in the normal direction corresponds to the vasodilation. By using this model, the artery dilation at a particular point in time can be retrieved through an affine registration between the image at that time and an image used as reference. Despite solving many problems of previous approaches, with this method there are still some situations that can lead to misregistration between frames which include the presence of either adjacent vessels due to probe movement or muscular fascias and fibres, and poor image quality.

Since its introduction by Viola[2] and Collignon,[3] mutual information has become the standard similarity metric used in most of registration schemes. However, the selection of pixel intensity as the feature to match a pair of images is seldomly questioned. Intuitively, one would expect to have better results if more spatial information was used at each pixel position. Accordingly, previous works have been presented in which other features are introduced in the similarity measure.[4–8]

The main problem with estimating mutual information on high dimensional features is that histograms cannot be used to estimate probability density functions (pdf) due to the curse of dimensionality problem. To cope with this problem, Neemuchwala *et al.*[9] proposed a direct α-MI estimator that completely bypasses the pdf estimation,

Further author information:
E-mail: estanislao.oubel@upf.edu; phone: +34 93 542 1446; fax: +34 93 542 2517; web: http://www.cilab.upf.edu

thus overcoming the curse of dimensionality associated with using high dimensional histograms. Recently, the same authors[10] applied this method to the registration of breast ultrasound images using an ICA decomposition of subimages (patches) as feature vectors. In this this study, only rigid transformations were considered in the experiments.

In this work, we have investigated the registration performance of affine registration in FMD sequences when both NMI and α-MI are used. The use of spatial information in this particular application is expected to achieve more robust results in the presence of structures that can typically be misinterpreted as vessel walls, subsequently leading to incorrect alignments. A second purpose of this work is to validate the method proposed by Hero *et al.*[8] on a data set for which both manual dilation measures and automatic dilation measures obtained with NMI-based registration are available. In the context of this paper, the term NMI will always imply the use of pixel intensity as feature, while general d-dimensional feature vectors will be used with α-MI.

This paper is organized in seven sections. Section 2 presents the concept of α-MI and explains how to estimate it using kNN graphs. The problem of identifying which features should be used with α-MI is also addressed and the ICA model used in this work is explained. The method proposed by Frangi *et al.* for artery dilation assessment is illustrated in Section 3. Section 4 describes the procedure applied to process the FMD sequences, and the obtained results and corresponding discussion are presented in Sections 5 and 6, respectively. Finally, the conclusions can be found in Section 7.

2. α-MI ESTIMATION

2.1. Definition

Let I_s and I_t be random variables representing the source and target image, with pdfs $p_s(I_s)$ and $p_t(I_t)$ respectively. Let $p_{st}(I_s, I_t)$ represent the joint pdf of I_s and I_t. If the images were identical, I_s and I_t would be completely dependent random variables. On the other hand, if the images were statistically independent, the joint pdf between I_s and I_t would factor into the product of the corresponding marginal pdfs $p_{st}(I_s, I_t) = p_s(I_s)p_t(I_t)$. This suggests the use of α-divergence $D_\alpha(p_{st}(I_s, I_t)\|p_s(I_s)p_t(I_t))$ between $p_{st}(I_s, I_t)$ and $p_s(I_s)p_t(I_t)$ as a similarity measure. For $\alpha \in (0, 1)$ this divergence is called α-mutual information (or α-MI) of I_s and I_t and has the form

$$\begin{aligned} \alpha MI &= D_\alpha(p_{st}(I_s, I_t) \parallel p_s(I_s)p_t(I_t)) \\ &= \frac{1}{\alpha - 1} \log \int p_{st}^{\alpha}(I_s, I_t) p_s^{1-\alpha}(I_s) p_t^{1-\alpha}(I_t) dI_s dI_t. \end{aligned} \tag{1}$$

When $\alpha \to 1$, α-MI converges to the standard (Shannon) MI

$$MI = \int p_{st}(I_s, I_t) \log \left(\frac{p_{st}(I_s, I_t)}{p_s(I_s)p_t(I_t)} \right) dI_s dI_t. \tag{2}$$

According to Equation (1), α-MI can be interpreted as a measure of dependency between variables I_s and I_t, which is expected to be maximum at registration.

2.2. Entropic spanning graphs

Given a set $\mathcal{Z} = \{z_1, \ldots, z_n\}$ of n vectors in $\mathbb{R}^d$, minimal graphs spanning this set of vectors can be used to construct a strongly consistent estimator of entropy for pdfs without singular (Dirac delta) components. In particular, let the functional $L_\gamma(\mathcal{Z})$ be defined as:

$$L_\gamma(\mathcal{Z}) = \min_{e_{ij} \in T} \sum_{ij} \|e_{ij}\|^\gamma, \tag{3}$$

In Equation (3), $\gamma \in (0, d)$ is a real number, e_{ij} is the edge connecting the points z_i and z_j, $\| \cdot \|$ is the Euclidean norm, and T is a subset of all $\binom{n}{2}$ edges satisfying some restriction, and over which the minimization

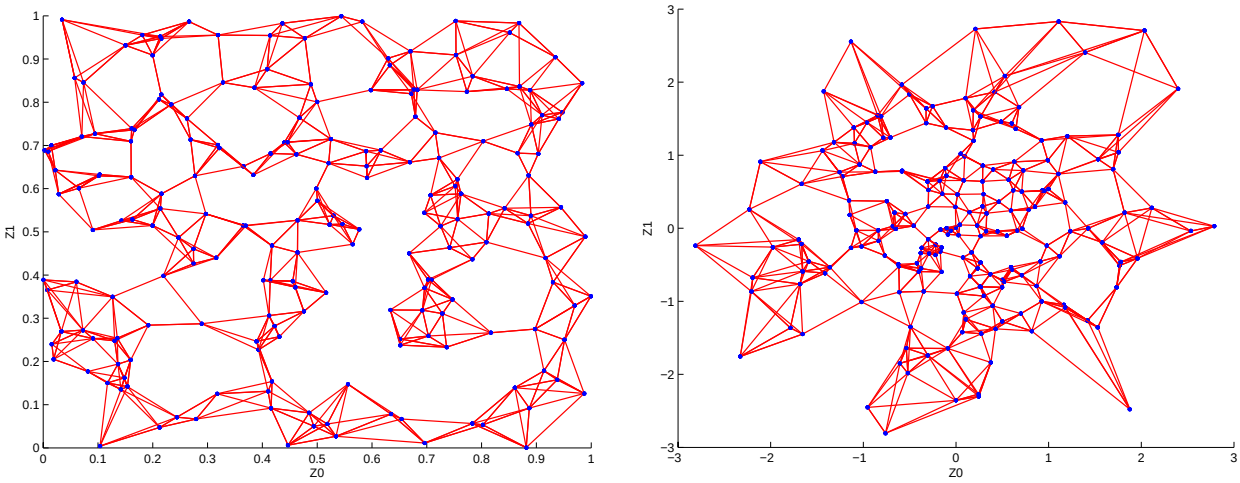

(a) (b)

Figure 1. kNN graphs for a set of 200 points in the plane and k=5. (a) uniform distribution (SD=1). (b) Gaussian distribution (SD=1).

is done. Depending on the choice of T, the obtained graph will be, for instance, a minimal spanning tree (MST), a Steiner tree (ST) or a travelling salesman problem (TSP) tree.

Hero *et al.* showed[11] that when a graph is quasi-additive in $\mathbb{R}^d$ and $d \geq 2$, the graph is an entropic spanning graph. Specifically,

$$H_\alpha(\mathcal{Z}) = 1/(1-\alpha)\left[\lim_{n\to\infty} \log L_\gamma(\mathcal{Z})/n^\alpha - \log \beta_{d,\gamma}\right] \tag{4}$$

is an asymptotically unbiased and almost surely consistent estimator for the α-entropy of the distribution. In Equation (4), $\alpha = (d-\gamma)/d$ and $\beta_{L,\gamma}$ is a constant bias correction that only depends on the graph minimization criterion, e.g. MST, ST or TSP, but is independent of the underlying pdf.

The k-nearest neighbor graph (kNN graph) is a noteworthy type of graph because it has the same convergence properties than the previously mentioned graphs but it is faster and easier to calculate. kNN graphs are formed by the points z_i and the edges with their k nearest points $\mathcal{N}_{k,i}(\mathcal{Z})$. Figure 1 shows two examples of kNN graphs for different distributions. The kNN length can be calculated as follows:

$$L_{\gamma,k}(\mathcal{Z}) = \sum_{i=1}^{n} \sum_{e\in\mathcal{N}_{k,i}} \|e\|^\gamma. \tag{5}$$

2.3. α-MI estimation

Let I_s and I_t be two images from which the sets of feature vectors $\mathcal{Z}_s = \{z_{s1}, \ldots, z_{sn}\}$ and $\mathcal{Z}_t = \{z_{t1}, \ldots, z_{tn}\}$ have been extracted. kNN graphs allow to estimate α-MI between these images as[9]

$$\widehat{\alpha MI} = \frac{1}{\alpha-1} \log \frac{1}{n^\alpha} \sum_{i=1}^{n} \sum_{p=1}^{k} \left(\frac{\|e_{ip}(z_{si}, z_{ti})\|}{\sqrt{\|e_{ip}(z_{si})\| \; \|e_{ip}(z_{ti})\|}} \right)^{2\gamma}, \tag{6}$$

where $\|e_{ip}(z_{si}, z_{ti})\|$ is the distance from the point $(z_{si}, z_{ti}) \in \mathbb{R}^{2d}$ to its p-nearest neighbor in $\{z_{sj}, z_{tj}\}_{j\neq i}$, and $\|e_{ip}(z_{si})\|$ ($\|e_{ip}(z_{ti})\|$) is the distance from the point $z_{si} \in \mathbb{R}^d, (z_{ti} \in \mathbb{R}^d)$ to its p-nearest neighbor in $\{z_{sj}\}_{j\neq i}(\{z_{tj}\}_{j\neq i})$.

2.4. Feature vectors

Although pixel intensity is the feature used in almost all MI based registration schemes, other features are also possible. As pointed out by Leventon and Grimson,[12] MI does not take into account joint spatial coherence of the pixels, which can improve the registration. Previous work has reported the use of features other than pixel intensity.[4, 13, 14]

There are many possible feature vectors that can be used with α-MI. An interesting alternative to pixel intensity is the use of an Independent Component Analysis (ICA) representation of subimages (patches) at different positions in the image. One advantage of using ICA is that each patch is represented by a vector of statistically independent components and therefore the hypothesis about independence and distribution of random variables is fulfilled by construction. In ICA, signals are considered as random variables x_i and are modelled as a linear combination of statistically independent random variables s_j as follows:

$$x_i = \sum_{j=1}^{p} a_{ij} s_j. \tag{7}$$

When modelling images with ICA, each x_i corresponds to a particular pixel position in the patch. Different realizations of these random variables are obtained by taking different patches. The matrix a_{ij} is known as the mixing matrix and its columns are the components of the basis. When using ICA, the independent components s_j define the feature vectors z_i.

3. ARTERY DILATION ASSESSMENT

The method proposed by Frangi *et al.*[1] to retrieve artery dilation assumes that the interframe vasodilation can be modelled by a constant scaling in the direction normal to the artery. Thus, the vasodilation existing between two frames can be obtained by an affine registration between these frames, and by taking the scaling factor in the y axis as the relative dilation. This method needs to define a reference frame with respect to which all the other frames are registered. In the original implementation, the reference frame was the first frame of the sequence. However, if the reference frame is defined as the one acquired 60 s after the cuff release, enhanced results are obtained in the clinically relevant part of the curve.[15] For this paper we took the last approach.

The original method removes background extra luminal structures by padding them out from the reference frame to avoid artifacts when measuring arterial vasodilation. Preprocessing of the reference frame also requires repositioning it so that the artery is normal to the scaling direction, i e., aligned with the horizontal axis since the model searches for a vertical scaling factor. The same image preprocessing was made in this work.

4. MATERIALS AND METHOD

4.1. Data set description

Two sequences corresponding to 2 members of the Spanish Army were studied. Figure 2 shows the reference frames corresponding to these sequences. This sample belongs to the AGEMZA cohort study of cardiovascular risk factors in young adults. Images were acquired at telediastole, coinciding with the QRS complex. A Sonos 4500 US scanner (ATL, Andover, CA, USA) in frequency fusion mode and a 5-7.5 Mhz trapezoidal multifrequency probe was employed. For each sequence of approximately 20 minutes and 1200 frames, two responses are acquired: FMD and nitroglycerine mediated dilation (NMD). Gold-Standard measurements derived from manual measurement by three experts were obtained in 56 frames from these sequences, in two independent sessions. Each manual measurement was performed fitting a spline model to each wall. FMD curves obtained with normalized mutual information are also available.

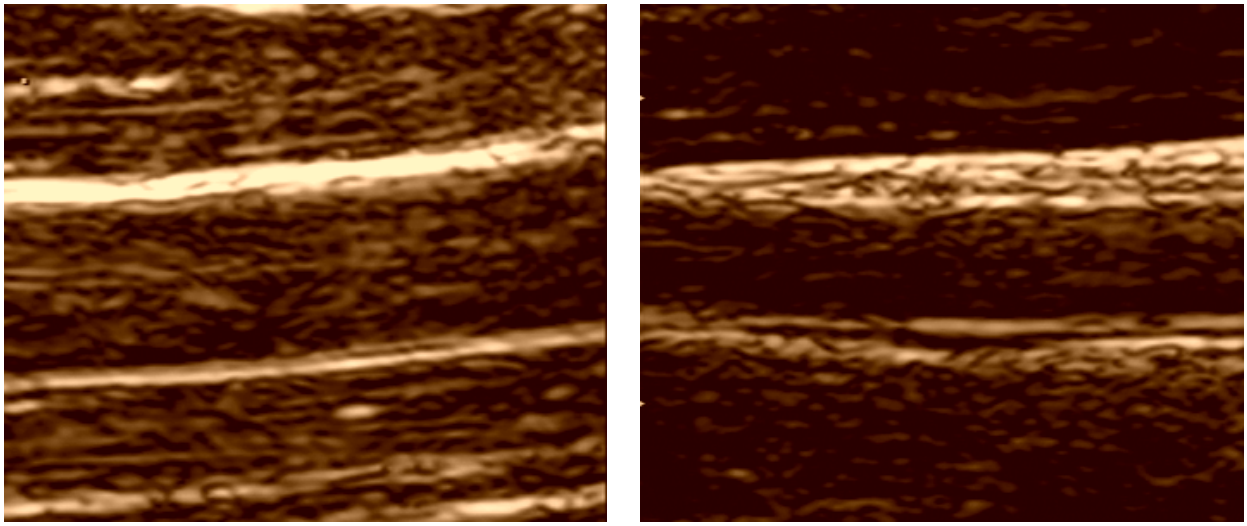

(a) (b)

Figure 2. Reference frames corresponding to the sequences used in this work. (a) sequence A. (b) sequence B.

4.2. Image registration method

The framework proposed by Studholme *et al.*[16] was employed to recover the optimal transformation. As the purpose of this work was to evaluate the benefits of using α-MI as similarity measure, the main modification to the method described in Section 3 was a change in the similarity metric used to compare the images. Specifically, NMI was replaced with α-MI of an ICA representation of patches at different positions in the image.

For each sequence, an ICA basis was generated using Hyvarinen and Oja's FastICA code.[17] Patches of size 16×16 pixels were taken from images at equally spaced positions as shown in Figure 3(a). To reduce the dimensionality, a Principal Component Analysis (PCA) was performed before the computation of ICA, and only the components necessary to explain up to 95% of variance were kept (6-8 components, depending on the sequence). Additional dimensionality reduction was obtained by blurring the images with a Gaussian filter before doing ICA (with the corresponding PCA preprocessing). To make the method consistent, the low-pass versions of the images were used in the registration instead of the original ones. Figure 3(b) shows two different basis obtained for two different values of variance.

For interframe registration, approximately $n = 8000$ feature vectors were extracted from the source and target frames. This was done taking a patch 16×16 every 4 pixels in each direction and multiplying them by the demixing matrix W calculated for each sequence. These feature vectors were used to estimate the α-MI using Equation (6) with $k = 20$ and $\alpha = 0.5$.

5. RESULTS

The accuracy of the method was evaluated by comparing the automatic measurements to the manual measurements made by experts. The arterial diameter was measured in 56 frames from the two sequences used to test the method. Three experts assessed each frame twice, in independent sessions, by fitting a spline to the inner contour of each vessel wall. The diameter was subsequently calculated as the average distance between these curves. More details about this method can be found in our previous work.[1]

The scaling factor in the direction normal to the vessel axis relating each frame to the reference frame constitutes the vasodilation output parameter of the automatic method. As a consequence, the automatic measurements are referred to the arterial diameter of the reference frame. To enable the comparison with the gold standard, the manual measurements were also divided by the dilation at the reference frame. As the comparison method we used Bland-Altman plots, which defines limits of agreement between two measurement

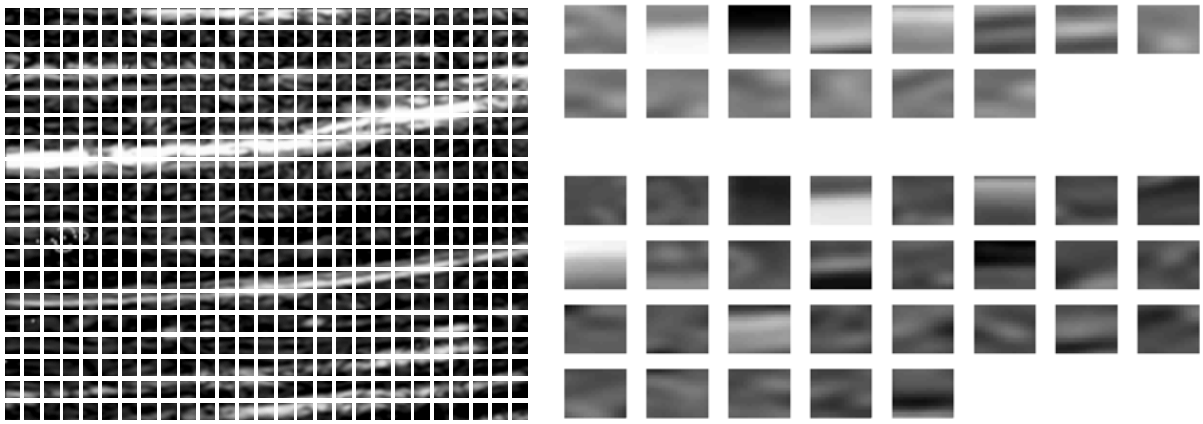

Figure 3. (a) Patches used for obtaining the ICA basis. (b) Components of the ICA basis for 99.0% (top) and 99.9% (bottom) of variance explanation.

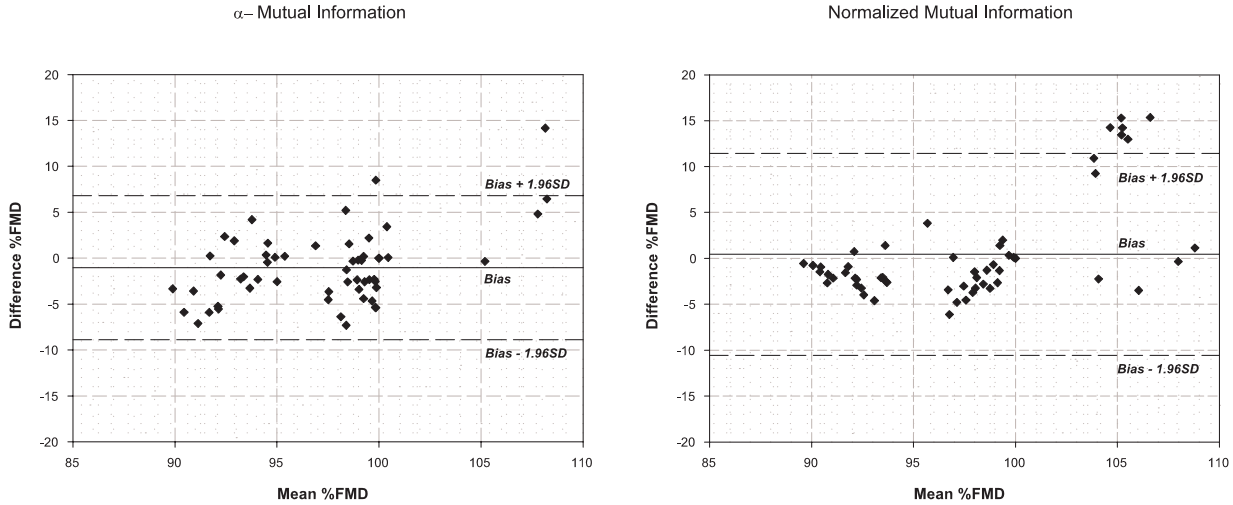

Figure 4. Bland-Altman plots comparing the automatic measurements using (a) α-MI, and (b) NMI versus the gold standard

techniques as indicated by $d = \pm 1.96SD$, where d is the mean difference (bias) and SD is the standard deviation of the differences.

Figure 4 shows a Bland-Altman plot comparing the automated versus the gold-standard measurements when using NMI and α-MI. Figure 5 presents the clinically relevant part of the dilation curves. The manual measurements have been superimposed onto the curves along with the 95% confidence interval for comparison. Even though the α-MI dilation curve for sequence A shows more local variations than the NMI curve, the method based on α-MI clearly exhibits better agreement with the gold standard at frames 351 and 401. Furthermore, the peak in the NMI curve at frame 432, which is caused by poor image quality of the sequence in that part, is not present in the curve obtained by using α-MI. In the rest of the frames assessed by the experts, α-MI performs similarly to NMI.

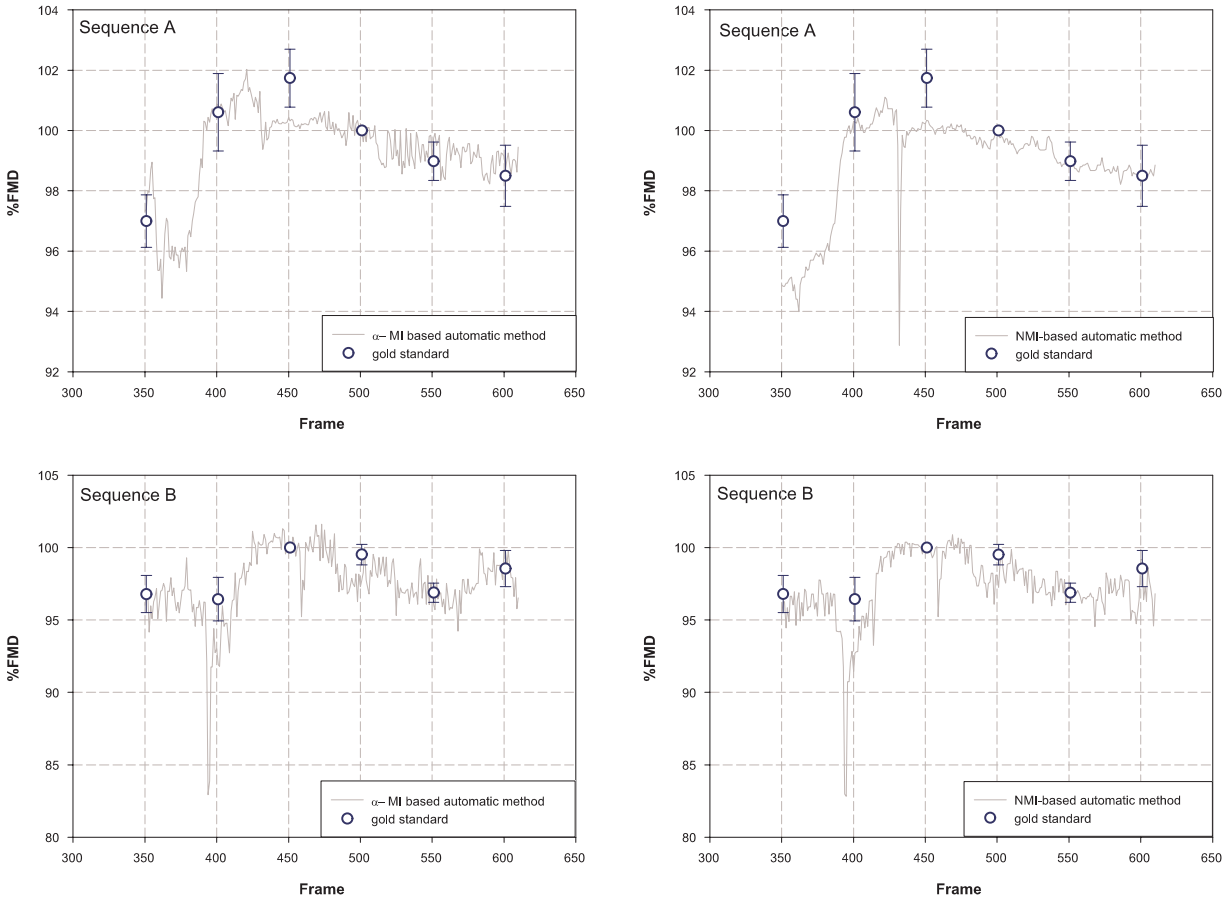

(a) (b)

Figure 5. FMD curves for both sequences obtained with the automatic method by using (a) α-MI and (b) NMI. Error bars show the 95% confidence interval of the gold standard measurements for comparison.

6. DISCUSSION

As can be deduced from Figures 4 and 5, for this particular application the performance of α-MI based on ICA feature vectors and NMI are similar. In this paper, a decomposition into independent components was used as feature vectors motivated by the dimensionality reduction and the assumptions on the random variables representing the images. However, many other alternatives are possible which make this method promising. A comparative study focusing on the relative benefits of different basis to discriminate local spatial features will be the subject of future work.

The bias observed from Figure 4 may derive from the normalization process. The manual measurements used as gold standard were made in order to minimize the error in the initial frames of the sequence. For this purpose, more measurements were made at the beginning of the sequence (phase B1) than in the other phases. In the work by Frangi *et al.*,[1] the dilation measurements were referred to the first frame and the manual measurements were normalized to the average in phase B1. In this work, the dilation was calculated with respect to a frame near to the dilation peak in the FMD phase and the manual measurements were normalized to the dilation corresponding to this frame. Thus, the comparison has a strong dependency on the accuracy of the manual measurement at this frame.

The use of the kNN graph estimator of α-MI introduces additional registration parameters whose influence in

the estimation accuracy needs further study. As pointed out by Neemuchwala *et al.*,[9] the convergence properties of the estimator in Equation (6) are currently unknown and should be also studied in depth. Furthermore, the influence of the feature used to match images deserves special consideration. Among the available options, the use of wavelets seems promising and will be the subject of future work.

The main disadvantage of using kNN graphs with respect to using histograms is the computational burden. In our experiments, making use of a Xeon microprocessor at 2.8 GHz CPU and 2 GB RAM running Fedora Core 2, the registration time for each sequence was 6 h for α-MI and 30 min for NMI. However, when using high dimensional features, the use of histograms is not an alternative because of the curse of dimensionality, and therefore, the computational complexity becomes meaningless. It is finally worth noting that the potential benefits of using α-MI should be balanced against its computational cost when choosing the measure of similarity for a particular application.

7. CONCLUSIONS

Entropic graph estimation of α-MI has been applied as similarity measure for registration of FMD sequences to evaluate the effect of including spatial information in this particular application. To the best of our knowledge, this is the first work in which spanning trees have been applied for affine registration of image sequences. The results showed that the performance of α-MI and NMI are comparable but the registration time was longer. However, this method is promising because it offers more flexibility with respect to the selection of features for matching the images. The choice of the registration parameters values (and, in particular, of the basis to obtain the feature vectors) deserves special consideration and will be the subject of future work.

ACKNOWLEDGMENTS

This work was partially funded by Red IM3: Imagen Médica Molecular y Multimodalidad (ISCIII G03/185), Redes Temáticas Colaborativas, Ministerio de Sanidad y Consumo de España (http://im3.rediris.es) and TIC2002-04495-C02 grant. The work of E. Oubel is supported by the Spanish Ministry of Education under a FPU Grant AP2003-1535. The work of A.F. Frangi is supported by the Spanish Ministry of Science and Technology under a Ramón y Cajal Research Fellowship. GridSystems S.A., Palma de Mallorca, Spain (http://www.gridsystems.com) is also acknowledged for providing the InnerGrid Nitya Middleware for grid computing and technical support. The authors are grateful to S. Ordás for his valuable support in the use of the grid computing facilities.

REFERENCES

1. A. Frangi, M. Laclaustra, and P. Lamata, "A registration-based approach to quantify flow-mediated dilation (FMD) of the brachial artery in ultrasound image sequences," *IEEE Transactions on Medical Imaging* **22**(11), pp. 1458–69, 2003.
2. P. Viola and W. M. Wells III, "Alignment by maximization of mutual information," in *Int. Conf. Computer Vision*, E. Grimson, S. Shafer, A. Blake, and K. Sugihara, eds., pp. 16–23, (Los Alamitos, CA), 1995.
3. A. Collignon, F. Maes, D. Delaere, D. Vandermeulen, P. Suetens, and G. Marchal, "Automated multi-modality image registration based on information theory," in *Information Processing in Medical Imaging*, Y.Bizais, C. Barillot, and R. D. Paola, eds., pp. 263–274, Kluwer Academic Pub, (Ile de Berder, France), June 1995.
4. D. Rueckert, M. J. Clarkson, D. L. G. Hill, and D. J. Hawkes, "Non-rigid registration using higher-order mutual information," *SPIE Medical Imaging: Image Processing, San Diego, CA* , pp. 438–447, 2000.
5. J. P. W. Pluim, J. B. A. Maintz, and M. A. Viergever, "Image registration by maximization of combined mutual information and gradient information," *IEEE Transactions on Medical Imaging* **19**(8), pp. 809–814, 2000.
6. D. B. Russakoff, C. Tomasi, T. Rohlfing, and C. R. Maurer, "Image similarity using mutual information of regions," *8th European Conference on Computer Vision (ECCV)* , pp. 596–607, 2004.

7. J. Zhang and A. Rangarajan, "A unified feature-based registration method for multimodality images," in *Proceedings of the 2004 IEEE International Symposium on Biomedical Imaging: From Nano to Macro, Arlington, VA, USA*, pp. 724–727, IEEE, April 2004.
8. A. O. Hero, B. Ma, O. Michael, and J. Gorman, "Applications of entropic spanning graphs," *IEEE Signal Processing Magazine (Special Issue on Mathematics in Imaging)* **19**(5), pp. 85–95, 2002.
9. H. F. Neemuchwala and A. O. Hero, *Multi-sensor image fusion and its applications*, ch. Entropic graphs for registration. Marcel-Dekker, Inc., 2004 (in press).
10. H. F. Neemuchwala, A. O. Hero, and P. L. Carson, "Image registration using alpha-entropy measures and entropic graphs," *European Journal on Signal Processing (Special Issue on: Content-based Visual Information Retrieval)* , (in press).
11. A. O. Hero and O. Michael, "Asymptotic theory of greedy approximations to minimal k-point random graphs," *IEEE Transactions on Information Theory* **45**(6), pp. 1921–1939, 1999.
12. M. E. Leventon and W. E. L. Grimson, "Multi-modal volume registration using joint intensity distributions," in *MICCAI '98: Proceedings of the First International Conference on Medical Image Computing and Computer-Assisted Intervention*, pp. 1057–1066, Springer-Verlag, 1998.
13. T. Butz and J.-P. Thiran, "Affine registration with feature space mutual information," in *MICCAI '01: Proceedings of the 4th International Conference on Medical Image Computing and Computer-Assisted Intervention*, pp. 549–556, Springer-Verlag, 2001.
14. H. Neemuchwala, A. Hero, and P. Carson, "Feature coincidence trees for registration of ultrasound breast images," in *Proc. of IEEE Int. Conf. on Image Proc*, (Thesaloniki, Greece), October 2001.
15. L. Boisrobert, M. Laclaustra, M. Bossa, A. G. Frangi, and A. F. Frangi, "Combined statistical analysis of vasodilation and flow curves in brachial ultrasonography: Technique and its connection to cardiovascular risk factors," The International Society for Optical Engineering (SPIE), February 2005.
16. C. Studholme, D. L. G. Hill, and D. J. Hawkes, "An overlap invariant entropy measure of 3d medical image alignment," *Pattern Recogn.* **32**, pp. 71–86, 1999.
17. A. Hyvarinen and E. Oja, "FastICA," 1999. Available at http://www.cis.hut.fi/projects/ica/fastica/.